Fine structure of transverse modes in optical cavities

Bijl, Martin

Fine structure of transverse modes in optical cavities

THESIS

submitted in partial fulfillment of the
requirements for the degree of

BACHELOR OF SCIENCE
in
PHYSICS

Author :	Martin Bijl
Student ID :	
Supervisor :	Corné Koks
	Martin van Exter
Second corrector :	Wolfgang Loeffler

Leiden, The Netherlands, July 7, 2021

Fine structure of transverse modes in optical cavities

Martin Bijl

Huygens-Kamerlingh Onnes Laboratory, Leiden University
P.O. Box 9500, 2300 RA Leiden, The Netherlands

July 7, 2021

Abstract

We study the fine structure of transverse modes of an optical micro cavity. We measure the transmission of a 633 nm He-Ne laser as a function of the cavity length, from which we can extract the mirror radius of curvature, the well known paraxial shifts, and higher-order corrections. The goal is to distinguish between fine structure caused by non-paraxial effects and mirror related effects. We find that the resonant cavity lengths predicted by the non-paraxial model is only correct for certain resonant modes. We also measure the mirrors with an AFM and find that mirror related effects are small compared to the non-paraxial effects. Further investigation with a polarization-resolving CCD camera reveals that the polarization profiles of transverse modes are similar to what the non-paraxial theory predicts, but it also shows that the occurrence of almost all modes is shifted. The experiment suggests that the models are good, but insufficient to fully describe the fine structure of a Fabry–Perot interferometer.

Contents

1 Introduction **7**

2 Theory **9**

3 Setup **11**

4 Transmission Spectra **13**
4.1 Voltage to Nanometer 13
4.2 Arcsine fit 15

5 Fine structure **17**
5.1 The fundamental mode 17
5.2 18 micron cavity 21
5.3 5 micron cavity 23
5.4 Discussion 25
5.4.1 Uphoff 25
5.4.2 Luk 26

6 CCD images **27**
6.1 Introduction 27
6.2 Setup 28
6.3 Results 29
6.4 Discussion 35

7 Atomic Force Microscope **37**
7.1 Methods 38
7.2 Results 39
7.3 Discussion 39

Version of July 7, 2021– Created July 7, 2021 - 19:45

8 Concluding Discussion **41**

Chapter 1

Introduction

One of the most fundamental concepts in physics is the harmonic oscillator. In optics one way to make an optical harmonic oscillator is by placing two mirrors in front of each other. Light that enters this system can bounce back and forth. Such a device has many practical applications [11] and is called a Fabry Pérot interferometer. For specific distances between the mirrors, a resonance between both mirrors will occur. We measure these resonances as a peak in the transmission while we change the distance between both mirrors. Each of these resonances can be labeled by a longitudinal index q and a transverse index N. The cavity length difference between q and $q+1$ (for N=-1) is called a free spectral range, and is in our research $\Delta L_{FSR} = \frac{\lambda}{2} = \frac{633}{2}$ nm. The paraxial approximation of a plano-concave cavity shows that the resonances only depends on the index q and N. However, close examination shows that the cavity length of resonances are not degenerate: For a q and N there are multiple peaks. This means that the two indices q and N are not enough to describe all resonances in a Fabry Pérot interferometer. We call these effects non-paraxial effects.

This is similar to quantum mechanics where the quantum number n in the Bohr model is not enough to describe all energy levels. The consequence of this is the existence of *fine structrue*. Similarly, the additional resonance in a Fabry Pérot interferometer can also be interpreted as fine structure. There are two sets of indices to describe the fine structure: n and m in the Hermite-Gaussian base and p and ℓ in the Laguerre-Gaussian base. The relation of these indices to N is $N = n + m = 2p + |\ell|$. The number of possible n and m or p and ℓ for N is $N + 1$. The non-paraxial effects prefer Laguerre-Gaussian modes [12], mirror related effects prefer Hermite-Gaussian modes [2].

In addition to the previously mentioned fine structure, there is also ad-

Version of July 7, 2021– Created July 7, 2021 - 19:45

ditional fine structure due the breaking of symmetry of the mirrors. The mirror effects we specifically look for is astigmatism. A mirror has astigmatism if the radius of curvature across one axis is different from another axis. Astigmatism causes a lifting of degeneracy of modes. The paper by Uphoff [3] predicts the distance between the lifted fundamental (N=0) mode. A splitted fundamental mode can have determent effects on experiments that rely on the fundamental modes [3] [5]. There are more mirror effects. [6] [4], but in this thesis we will only focus on astigmatism.

The goal of this research is do identify both sources of fine structure and check if the predicted fine structure conform with the experiment.

The thesis is structured as followed: We start in chapter 2 with a brief overview of the different theories that attempt to describe the fine structure. The next chapter describes the setup of the experiment. In following chapter 4 we show how the raw transmission spectra is processed into analysable data. Chapter 5 contains an analysis of the splitting of modes. In the next chapter we show the CCD pictures with polarization profiles of these modes. In chapter 7 we show the results of the the Atomic Force Microscope measurements of the mirrors. And chapter 8 is the final discussion where we compare the results from the transmission analysis and the AFM data.

Chapter 2

Theory

For a planar mirror cavity, resonance occurs when a plane wave fits between the mirrors. When the transmission is measured against the distance between the mirrors, resonance peaks occur for every half wavelength. In this experiment one of the mirrors is spherical instead of flat. A good approximation to describe the in-cavity light wave for this setup is the paraxial approximation. One can derive the Gaussian beam as a solution to the paraxial wave equation [9]. The resonant cavity length according to the paraxial theory of each N is given by equation (2.1) [10] [1].

$$L = \frac{\lambda}{2}\left(q + \frac{N+1}{\pi}\arcsin\sqrt{\frac{L}{R}}\right) \tag{2.1}$$

Where λ the wavelength, L is the cavity length, and R the radius of curvature of the spherical mirror. The arcsin factor is called the Gouy phase [10]. N is equal to $n + m$ for Hermite-Gaussian modes or $2p + \ell$ for Laguerre-Gaussian modes. The Hermite-Gaussian modes are higher-order transverse modes that exist, because the paraxial wave equation is a separable equation in x and y. The Laguerre-Gaussian modes are higher-order transverse modes that exist, due to radial and azimuthal symmetry [9].

Equation (2.1) predicts a frequency degeneracy for every N. Accurate measurements however detect the lifting of degeneracy in the same (q, N) group. The reason is that the paraxial approximation breaks down for small cavity length. These effects are called non-paraxial effects. The paper by Luk [8] uses perturbation theory to get a result to explain these additional peaks. The equation given by Luk is equation (2.2).

$$\nu = \frac{c}{2L}\left\{q + \frac{2p+\ell+1}{\pi}\arcsin\sqrt{\frac{L}{R}} + \frac{1}{8\pi kR}g(p,\ell)\right\} \tag{2.2}$$

Where c is the speed of light, $k = \frac{2\pi}{\lambda}$ is the wave number, and p and ℓ are respectively the radial and azimuthal index of the Laguerre-Gaussian modes. The integer $g(p,\ell)$ can also be written to $g(N,\ell)$ where $N = 2p+\ell$ and is equal to equation (2.3).

$$\begin{aligned} g(p,l) &= 2p^2 + 2p\ell - \ell^2 + 2p + \ell \pm 4\ell - 2 \\ g(N,l) &= \frac{1}{2}(N+1)^2 - \frac{3}{2}(\ell^2-1) - 4 \pm 4\ell \end{aligned} \tag{2.3}$$

$g(N,l)$ has two sets of resonances depending on the sign of the 4ℓ term. We call the resonances with a $+4\ell$ term A modes, and -4ℓ term B modes.

Besides non-paraxial effects, there are also effects due to astigmatism. Astigmatism breaks a symmetry in the system which causes a degeneracy to be lifted. This means more resonances. The paper by Uphoff et al. [3] discusses the effects of astigmatism of the two fundamental (N=0) peaks. The equation that is given by Uphoff's paper is equation (2.4). Equation (2.5) is the same equation but the splitting is in nano meter.

$$\delta\nu_x - \delta\nu_y = -\frac{c}{4\pi kL}\frac{R_1 - R_2}{R_1 R_2} \tag{2.4}$$

$$\Delta L \approx \frac{\lambda}{2\pi k}\frac{\Delta R}{R_{av}^2} = \frac{\lambda}{2\pi k R_{av}}\eta \tag{2.5}$$

In equation (2.4) R_1 and R_2 are respectively the largest and the smallest radii of curvature of the mirror. Then take the Taylor approximation of the right hand side assuming $\Delta R = R_1 - R_2$ is much smaller than $R_{av} = \frac{R_1+R_2}{2}$. This results in equation (2.5) where $\eta = \frac{\Delta R}{2R_{av}}$ a dimensionless constant that contains the level of astigmatism. Note that if there is no astigmatism, $\eta = 0$, then there is no distance between both N=0 peaks. Also note that equation (2.2) and equation (2.5) have both a prefactor of $\frac{1}{kR}$. However, since $g(N,l)$ always returns integers and η is typically in the order of 0.1, the distance between the fine structure predicted by Luk is larger than the distance between the fine structure predicted by Uphoff.

Version of July 7, 2021– Created July 7, 2021 - 19:45

Chapter 3

Setup

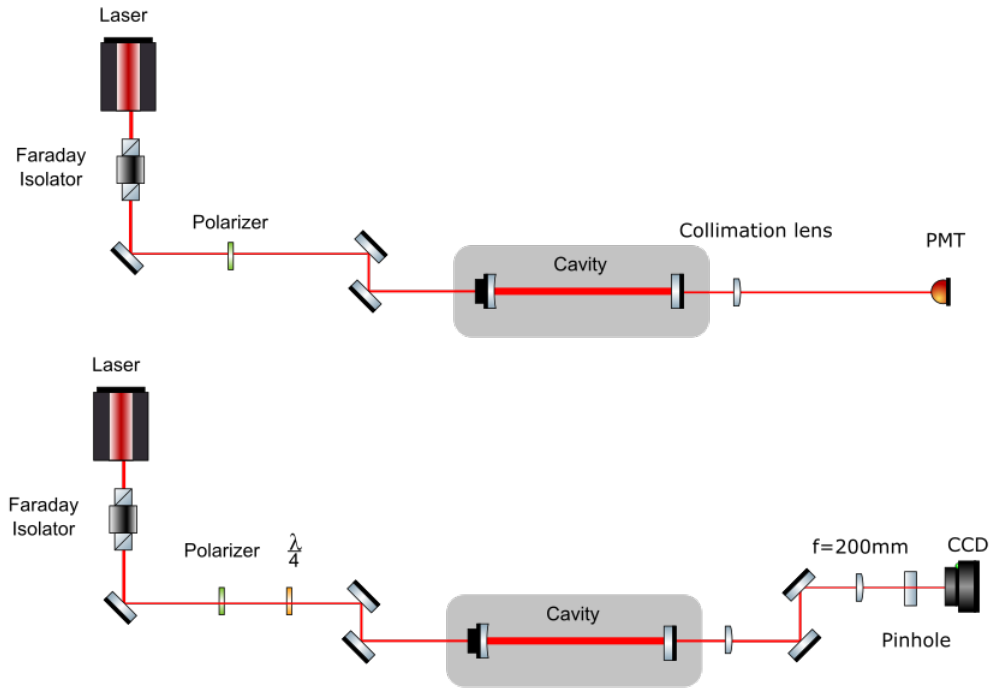

Figure 3.1: *The setup of this experiment. The top setup was used to measure the transmission spectra, the bottom setup was used to make the CCD figures.*

Figure 3.1 shows the setup that is used in this experiment. The laser beam is produced by a frequency stabilized 633 nm He-Ne laser. This beam first goes through an isolator to avoid feedback from light reflected from the cavity into the laser. Following this is is a polarizer. Then a periscope leads the beam into the cavity. The cavity contains two mirrors (DBRs), a concave one and a planar one. The concave mirror is a substrate with multiple mirrors with different radii of curvature. The planar mirror is connected to a piezoelectric element that expands when a higher voltage is applied. This causes the cavity to become shorter. A mirror below the cavity leads the beam into a photon multiplier tube that measures the intensity of the beam. The values are saved on the computer as a function of the voltage applied to the piezoelectric element. We used the second setup in figure 3.1 to determine the mode profiles and this is further discussed in the 'setup' section in chapter 6.

Version of July 7, 2021– Created July 7, 2021 - 19:45

Chapter 4

Transmission Spectra

A typical transmission spectrum looks like figure 4.1. The transmission is a function of the voltage applied on the piezoelectric material.

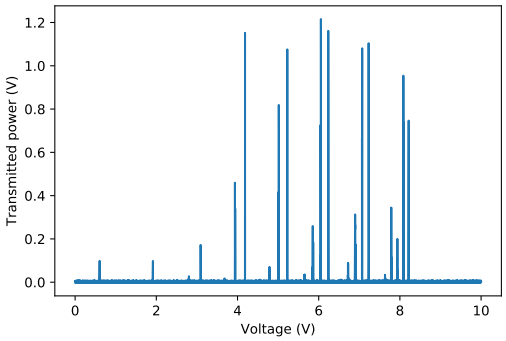

Figure 4.1: *Typical transmission spectrum as function of voltage. Higher voltage means shorter cavity length. This spectrum must therefore be read from right to left.*

4.1 Voltage to Nanometer

The x-axis of figure 4.1 is in voltage, but to compare with theory we like to convert voltage to cavity length. To do this, we use equation (2.1 to calculate the distance between two fundamental modes ($N = 0$, $q_1 \neq q_2$). Note that even for N=0, there is still a Gouy phase that depends on L, so the distance is more than just $\frac{633}{2}$. The distance between fundamental modes is expressed in equation (4.1).

$$\Delta d = \frac{\lambda}{2}\left(1 + \frac{1}{\pi}\arcsin\sqrt{\frac{L_{q+1}}{R}} - \frac{1}{\pi}\arcsin\sqrt{\frac{L_q}{R}}\right) \tag{4.1}$$

Where Δd is the cavity length difference between two fundamental modes and L_q the actual cavity length at the fundamental mode. This equation produces a list of the distances between fundamental peaks for multiple q. We then plot all distances of fundamental peaks on the y-axis starting at cavity length $L = 0$. Please note that d is not the actual cavity length L, there is an offset here that is discussed in the next section. The real cavity length is $L = L_0 + d$ where L0 is an offset. With the transmission spectra we correlate the cavity length of every fundamental peak with the voltage of every fundamental peak. Figure 4.2a shows how this looks like. This figure shows a correlation that is not linear. The reason is that the piezoelectric element reacts slowly to a change in the slope of the applied voltage. The physical fit of the piezoelectric element has the shape $d = aV + Ce^{-bV+d} + V$. The third-order Taylor approximation of d is a third degree polynomial. We use 4 fit parameters and fit 8 fundamental peaks as seen in figure 4.2a. The fit transforms the voltage into position for the entire transmission spectrum. We then calculate the residue of the fit by subtracting the predicted positions and the actual positions of fundamental modes and come to the conclusion that the residue is about 0.8 nm. Since we are only measure distances, the error is equal to $2 * 0.8 * \frac{2}{633} \approx 0.5\%$. The errors we measured when analysing the fine structure are an order of magnitude larger, therefore we conclude that this fit is good enough to analyse fine structure

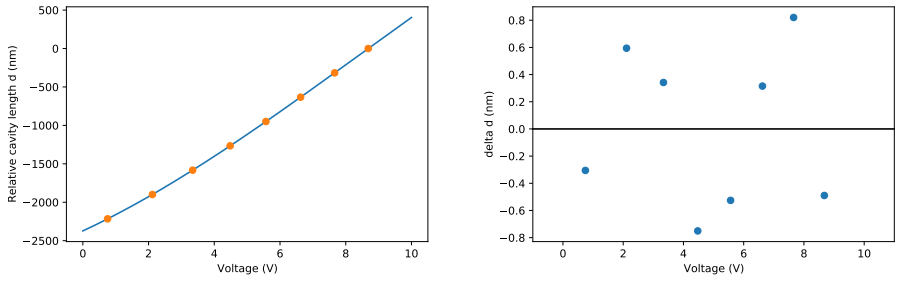

(a) ***(b)***

Figure 4.2: *Changing the x-axis from voltage to distance. Figure 4.2a shows the expected position of N=0 peaks in nm against measured positions in V. Figure 4.2b shows the residue of the fit: The expected positions of the N=0 peaks subtracted from the fit.*

4.2 Arcsine fit

In the previous section it was mentioned that the first fundamental mode has a cavity length of $0 + L_0$. L0 is an offset that contains information about the mirrors and what the actual index q of the fundamental mode is. In the paper by Koks [7] a method is discussed to find this offset and also the radius of the mirror. First plot the distance between a fundamental and higher order peak, such as N=1, and plot this against cavity length. Then take equation (4.2) as a fitting function, where the total offset L_t, and the radius of curvature R are parameters. Note that this is the same equation as (2.1)

$$\Delta d = \frac{\lambda}{2}\left(\frac{1}{\pi}\arcsin\sqrt{\frac{d+L_t}{R}}\right) \tag{4.2}$$

L_t is the x-coordinate where the Δd is equal to zero. L_t itself is equal to $L_t = L0 + 2L_D$, where L0 is the physical cavity length offset and L_D is the penetration depth of both mirrors. The nominator in the square root in equation (4.2) can be rewritten to $d + L_t = d + L0 + 2L_D = L + 2L_D$, where L is the actual cavity length. The rewritten equation is given by equation (4.3).

$$\Delta d = \frac{\lambda}{2}\left(\frac{1}{\pi}\arcsin\sqrt{\frac{L+2L_D}{R}}\right) \tag{4.3}$$

The 18 micron mirror has an L_t of $1.81(\pm 0.03)$ µm and an R of $18.1(\pm 0.2)$ µm. Then $L0 = 5 * \frac{\lambda}{2} = 1.58$ µm. So the first fundamental peak we measure, noted as q*=0, is equal to q=5. Then q*=1 is equal to q=6, and so on. L_D tells something about the penetration depth of the DBR. In case of the 18 micron mirror the difference is 0.23 µm. This means that the penetration depth of the DBR of the spherical mirror is $L_D = 0.11$ µm. This is really high, the paper suggests this depth should be about 0.04 µm [7].

Figure 4.3 shows the distance between N=0 and N=1 peaks plotted against the position. This is done for N=1 modes, but a similar plot can be made with N=2, 3 and higher order modes.

Version of July 7, 2021– Created July 7, 2021 - 19:45

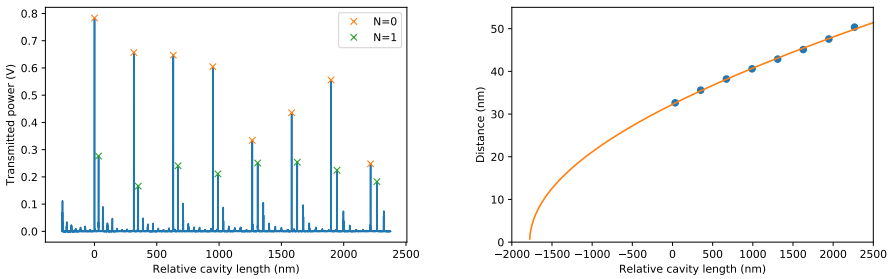

(a) ***(b)***

Figure 4.3: *Figure 4.3a shows several N=0 and N=1 resonances. The distance between the resonances are plotted against the distance in figure 4.3b. Then an arcsine function is fitted to the distances.*

Chapter 5

Fine structure

We measured a total of four different datasets. One measurement was done on a 18 micron cavity, three more measurements were done on a 5 micron cavity. We call the 18 micron cavity just the 18 micron measurement, the 5 micron cavity measurements we call measurement 5g (5 µm gom), 5f (5 µm fast), and 5s(5 µm slow). The 18 measurement is the overall best measurement, as it contains 8 fundamental peaks and contains many groups of transverse mode with a clearly visible fine structure with limit noise. Of the 5 micron cavity: Measurement 5g is a small cavity length measurement that has a very clear splitting of fundamental modes. Measurement 5g has only 5 fundamental peaks because it had gum in the cavity to decrease vibration noise. Its higher-order modes lose transmission fast: N=2 is hard to detect and even N=1 is not distinguishable after q*=3. This is due to the low overall transmission of this cavity due to the presence of a polarized beam splitter behind the cavity. This PBS is *only* used for measurement 5g. Measurement 5f and 5s are respectively very fast (0.1 s) and very slow (1.0 s) measurement on a 5 micron cavity. They both have 8 fundamental peaks. Unfortunately higher order modes die out fast for higher q, so it has just 4 usable free spectral ranges for fine structure analysis. Due to the slow measurement speed, measurement 5s data also has a lot more mechanical artifacts than the two previous mentioned measurements.

5.1 The fundamental mode

The fundamental mode, or the N=0 mode, is the first mode in a free spectral range and often has the highest transmission. It is a special mode,

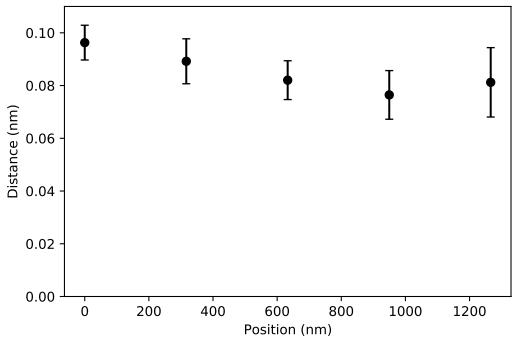

Figure 5.1: *Distance between fundamental peaks for five free spectral ranges of measurement 5g. The average distance is* $0.085\ (\pm 0.02)$ *nm.*

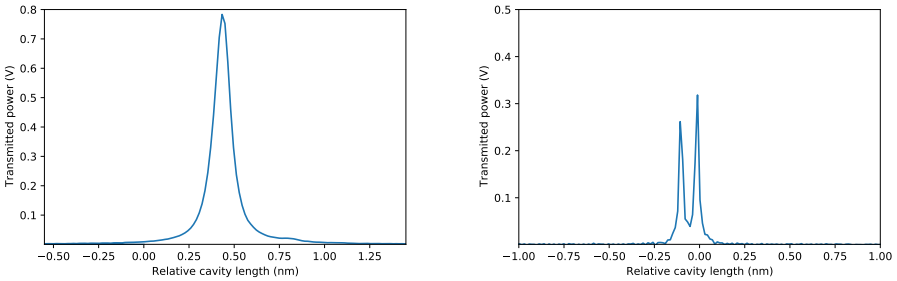

(a) *18 µm*

(b) *5µm g*

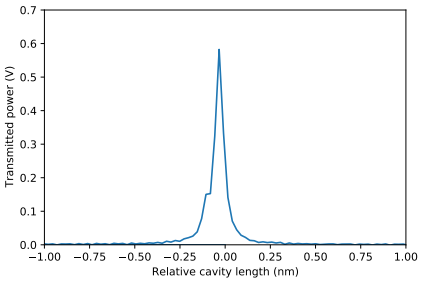

(c) *5µm f*

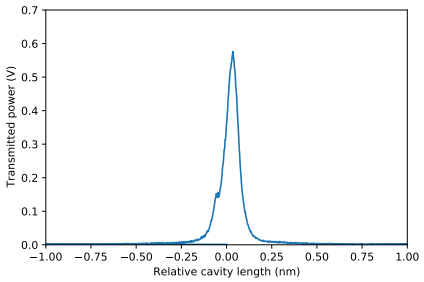

(d) *5µm s*

Figure 5.2: *Transmission spectra of N = 0, q*=0 of all four measurements. The cavity length domain for all figures is 2 nm. Only the 5g measurements in figure 5.2b shows a clear splitting of the fundamental modes*

because it has no degeneracy according to Luk. This is confirmed by most measurements. However, measurement 5g show a clear lifting of degeneracy for the fundamental mode. Figure 5.2 shows transmission spectra of the N=0 modes of multiple measurements. The theory in the paper of Uphoff indeed predicts a splitting if there is astigmatism in the spherical mirror.

The distance between both peaks is in the order of 0.1 nm and is hard to measure. The first reason is that the distance between both peak decreases as the astigmatism decreases. So good mirrors will not show any double peak. The seconds reason is that both peaks must have a large finesse or else the splitting will not meet the Rayleigh criterion and thus both peaks can not be distinguished from each other. The third reason is that it is easy to either scan too fast, so both peaks are seen as one peak or too slow so it is hard to distinguish a peak from noise.

We only found two peaks for N=0 in the 5g measurement. The disadvantage of this measurement is that it only has 5 free spectral ranges per run and N=1 is the highest mode that can be fully seen. Figure 5.1 shows the distance between both fundamental peaks. The average distance across all free spectral range is 0.085 (± 0.2) nm. Other experiments do not find a split fundamental peak, but it is possible to give an upper limit how large the splitting could be.

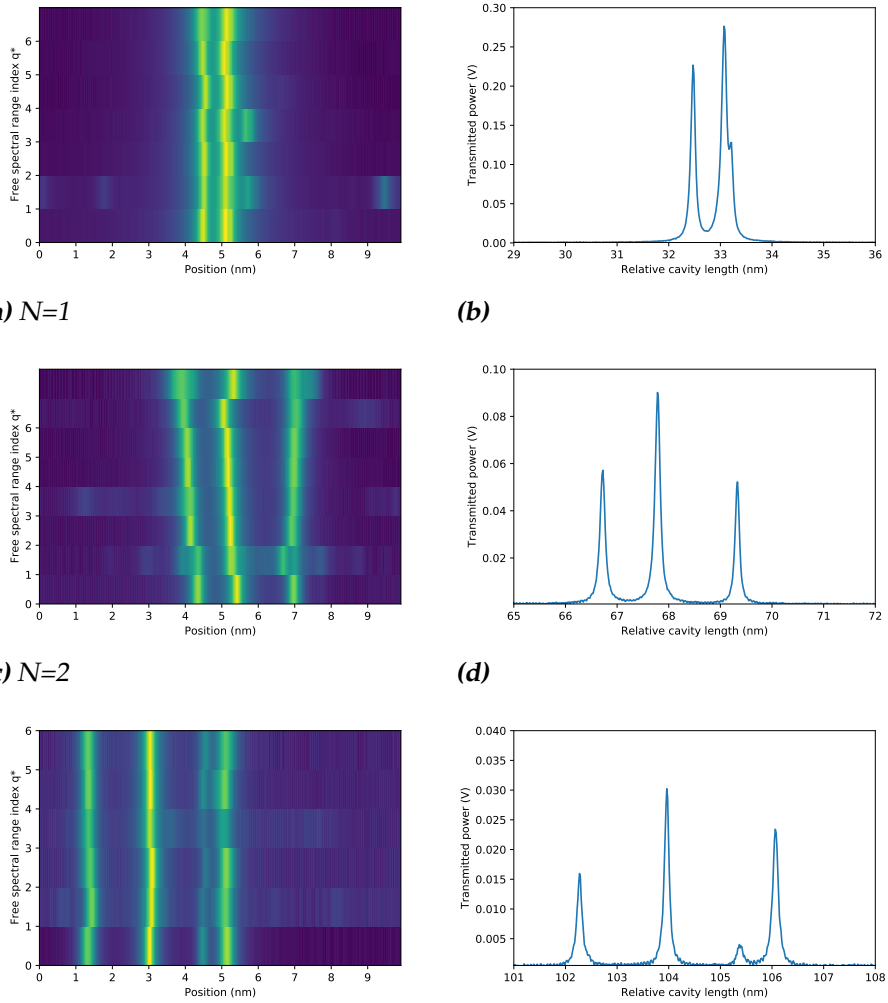

(a) *N=1* ***(b)***

(c) *N=2* ***(d)***

(e) *N=3* ***(f)***

Figure 5.3: *Transmission spectra of the N = 1, 2, and 3 group of the 18 micron measurement. Left are false color plots. The color shows the transmitted power, the x-axis is the relative distance and the y-axis is the free spectral range index q*. Right are the actual transmission spectra for q*=0 (q=5). The x-axis for these plots is the relative cavity length and has an offset of L0 =* 1820 *nm.*

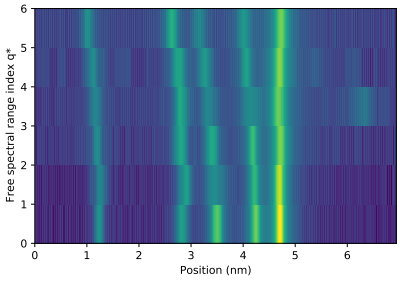

(a) *N=4*

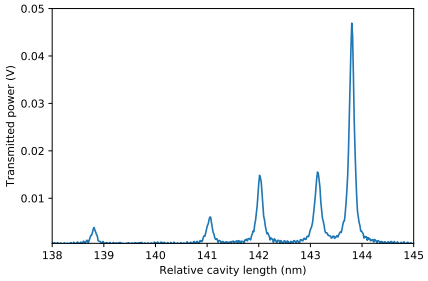

(b)

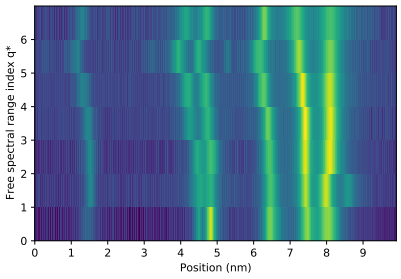

(c) *N=5*

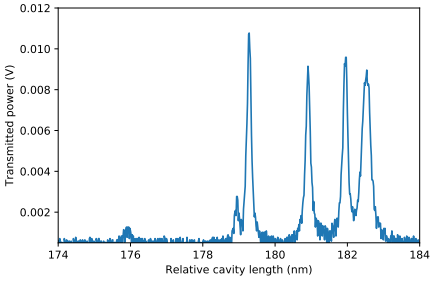

(d)

Figure 5.4: *Extention of figure 5.3, these plots are transmission spectra of the N = 4 and 5 groups.*

5.2 18 micron cavity

The 18 micron cavity measurement has the most expressed lifting of degeneracy.The following results are the average over at least 75 runs. Figure 5.5 shows how we created the average transmission: We calculated the average transmission by finding the highest transmission in the vicinity of a mode group. Then we shifted all transmissions by an offset, such that the data indices with the highest transmission were the same. Then we took the average transmission per measurement point and plotted the average. The average distances are calculated in a different way: We selected the same cavity length domain as before, then we found all peaks within this domain. We checked manually that every peak was selected, if this was impossible, then we excluded that run (this is why sometimes the average distance is over less than the 100 runs). In the next step we subtracted the cavity length of one mode with the previous mode. Then we took the average over all distances and calculate the standard deviation of all distances.

The researched modes are N=1 to N=5. We omitted higher modes than

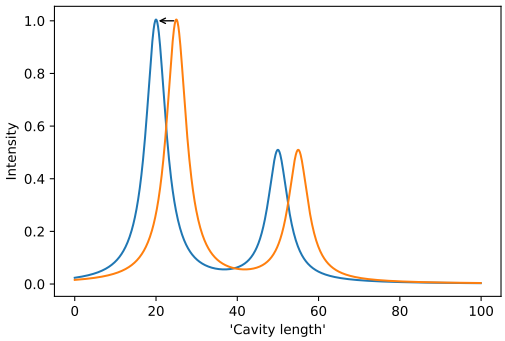

Figure 5.5: *This figure illustrates how the false color plots are created. First we find the global maximum of a selected domain. Then we shift all measurements, so the global maximum of all measurements has the same x-coordinate. Now we can take the average transmission as a function of the cavity length*

N=5, because not all N+1 peaks are visible due to noise.The following results are the average over at least 75 runs.

Figure 5.3b shows the transmission of the N=1 modes. The transmission spectrum shows two peaks that are 0.60 ($\pm$0.07) nm apart. Clearly visible on the right peak is the presence of a third peak 0.13 ($\pm$0.01) nm from the centre peak. All three peaks are visible and the distance remains the same for higher q. The false color plots show in figure 5.3a additional modes for q*=1 and q*=3, but these peaks are from N=9 modes at (q*-1) longitudinal mode number.

Figure 5.3d shows the transmission of the N=2 modes. It has three peaks, but q*=1 has more peaks. This is due to the N=10 modes from q*=0. In contrast to the N=1 modes, the distance between N=2 modes increase somewhat with higher cavity length as seen in 5.3c. The distance between peaks are from low to high cavity length and are 1.08 ($\pm$0.04) nm and 1.58 ($\pm$0.05) nm for q*=0. For q*=7 the distance has increased to respectively 1.11 ($\pm$0.06) nm, and 1.99 ($\pm$0.08) nm. The distance between the peaks on the left apparently does not increase for higher q, but the distance between the peaks on the right does.

Figure 5.3f shows the transmission of the N=3 modes. It has four peaks and like N=1 mode the distance between these peaks does not increase with higher q*. The average distance between peaks from left to right for q*=0 are 1.71 ($\pm$0.06) nm, 1.47 ($\pm$0.05) nm and 0.67 ($\pm$0.03) nm. For q*=5 the distances are 1.71 ($\pm$0.06) nm, 1.46 ($\pm$0.05) nm and, 0.59 ($\pm$0.03) nm.

The N=4 modes have five peaks as seen in figure 5.4b. The distance between peaks increases with higher cavity length, but, very slowly. The

average distance between peaks from left to right for q*=0 are 2.30 ($\pm$0.07) nm, 0.96 ($\pm$0.04) nm, 1.06 ($\pm$0.04) nm and 0.66 ($\pm$0.05) nm. For q*=5 the distances are increased to 2.36 ($\pm$0.08) nm, 0.75 ($\pm$0.04) nm, 1.17 ($\pm$0.05) nm, and 0.91 ($\pm$0.05) nm.

Figure 5.4b shows the transmission of the N=5 modes. The N=5 mode has six peaks. The distance between peaks increases with higher q*, but, with the exception of q*=5, slower than N=4. The average distance between peaks from left to right for q*=0 are 2.86 ($\pm$0.07) nm, 0.96 ($\pm$0.03) nm, 1.06 ($\pm$0.06) nm and 0.66 ($\pm$0.06) nm, and 0.87 ($\pm$0.03) nm.

In the discussion section, table 5.1 shows the distances in a compact way.

5.3 5 micron cavity

There are three different measurements that are done on a 5 micron cavity: Measurement 5g, 5f, and 5s. The low radius of curvature causes a large distance between peaks. Unfortunately the transmission of the higher-order modes is strongly reduced, so we could only distinguish modes N=1 and N=2.

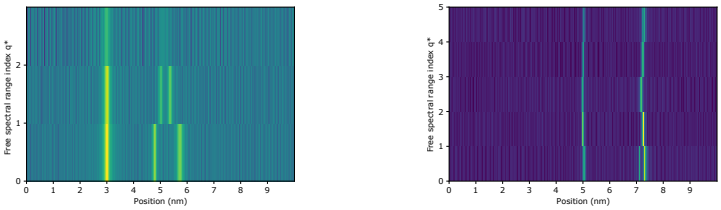

(a) *Measurement 5g* ***(b)*** *Measurement 5f*

Figure 5.6: *False color plots of N=1 modes of two measurements on a 5 µm cavity. Both measurements have a splitting on the right peak. But for higher q there are only two peaks. Also note how for higher q the positions of the two right peaks tends to converge to a position between the splitting for lower q.*

The N=1 modes are clearly visible in all measurements. All three measurements have three peaks for q*=0, one more than expected from Luk's theory. For q*=0, measurement 5g has a distance between the left and middle peak is 1.79 ($\pm$0.02) nm, the distance between the middle and right peak is 0.93 ($\pm$0.03) nm. However, both measurements 5f and 5s show a much smaller splitting on the right: 2.07 ($\pm$0.05) nm and 0.19 ($\pm$0.02) nm for measurement 5f measurement and 2.05 ($\pm$0.06) nm and 0.21 ($\pm$0.03)

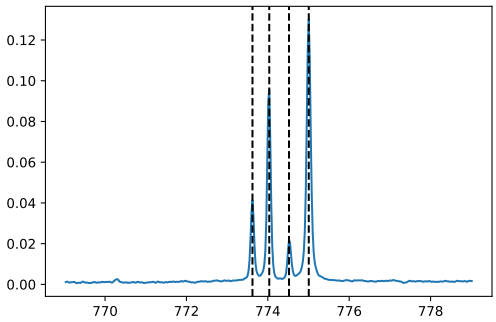

Figure 5.7: *N=2 modes of the 5 micron cavity for q*=3 (q=5). The four dashed lines show the four peaks. Note the additional small peak at 770 nm.*

nm for measurement 5s. For q*=1, measurement 5g still shows three peaks, but the right two peaks are closer now. The distance is 2.04 ($\pm$0.04) nm and 0.16 ($\pm$0.03) nm. The other two measurements 5f and 5s have just the two peaks expected by Luk. The distance between the peaks does not increase with cavity length and is for measurement 5f equal to 2.15 ($\pm$0.09) nm and for measurement 5s 2.14 ($\pm$0.19) nm for q* = 1, 2, 3 and 4. Note the increase in uncertainty for the slow measurement.

Figure 5.7 shows the transmission spectrum for N=2 of measurement 5f. The N=2 resonances of measurement 5g are too weak to distinguish from noise. The other two measurements, 5f and 5s, have visible N=2 modes. There are four clear peaks. In contrast to the N=1 mode, these peaks remain clearly separated for higher free spectral range. Also there is a fifth peak 3 nanometer to the left that is consistently always visible in multiple runs and multiple free spectral ranges. Unfortunately this resonance has so little transmission, it is hard to make out from the noise. The distance between the left double resonance is 0.37 ($\pm$0.03) nm, the right double resonance is 0.41 ($\pm$0.03) nm. The distance in between is 1.26 ($\pm$0.07) nm. The distance between the weak resonance on the left and the left major resonance is 3.24 ($\pm$0.04) nm. However, this is an average over 10 runs, not 50 runs like the previous mentioned distances.

The measurement 5s has too much noise and too many artifact to detect N=2 modes.

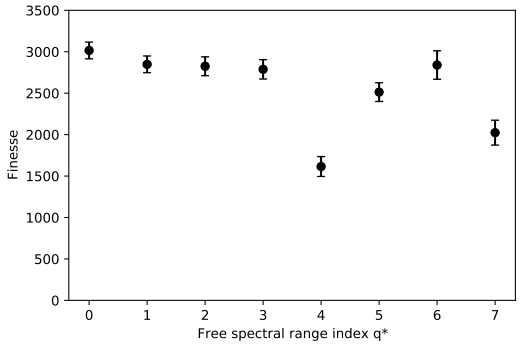

Figure 5.8: *The measured finesse of the N=0 peaks of the 18 micron mirror. The x-axis shows the free spectral range index q*. Note that q*=0 has an offset of q=5. The y-axis shows the finesse. The finesse drops for q*=4 (q=9), when the resonances of N=7 from q*=3 become frequency degenerate at the same cavity length as N=0 mode.*

5.4 Discussion

We noticed that the transmission spectra of measurement 5g and measurement 5f and 5s different (Figure 5.6). This suggests that the cavity of measurement 5f and 5s was not the same as measurement 5g. Measurement 5g is still useful to analyse the splitting of the N=0 modes. For higher order modes we use the 18 micron cavity.

5.4.1 Uphoff

Only measurement 5g is capable of measuring the fine structure in the fundamental mode caused by astigmatism. The distance between the fundamental peaks have a distance of 0.085 nm. We use equation 2.5 to calculate the astigmatism of the mirrors using the theory described by Uphoff [3]. For a cavity with average radius of 4800 µm, this equation returns $\eta = 0.04$, which means $\Delta R = 0.39$ µm.

Although the 18 micron measurement does not show two peaks for the fundamental modes, it is still possible to give a upper limit. We use the FWHM as an upper limit of this splitting. The finesse of the N=0 peaks is given in figure 5.8. For q=0, the finesse is $3000(\pm 100)$, this is a FWHM of 0.11 nm. Since the finesse stays the same for low q, the FWHM will not be much different for these q. We use equation (2.5) to calculate that $\Delta R \leq 7.0$ µm or $\eta \leq 0.19$. This is the upper limit that the astigmatism can be for the 18 micron mirror.

The	0-1	1-2	2-3	3-4	4-5
1	0.56				
2	0.97	0.14			
3	1.39	0.28	0.28		
4	1.81	0.42	0.56	0.14	
5	2.23	0.56	0.83	0.28	0.28

Exp	0-1	1-2	2-3	3-4	4-5
1	0.60				
2	1.08	1.58			
3	1.71	1.47	0.67		
4	2.30	0.96	1.06	0.66	
5	2.86	0.57	1.61	1.10	0.87

Table 5.1: *For the 18 micron cavity: The left table shows the distances (nm) between peaks that Luk predicts, the right table shows the distances we measured. The rows are the indices N, the columns are the distances between peak n and n+1, going from short to large cavity length.*

5.4.2 Luk

The fine structure is clearly visible for N=1 to N=5. Table 5.1 shows the theoretical and experimental values. For some modes, the distance is well predicted: Most distances between the 0th and 1st peak are close to what Luk predicts. However, other distances are way off: For example for N=2 the measured distance between the 1st and 2nd peak is off by one order of magnitude. It is curious that the distances for some modes are excellent predicted, but for other peaks the distance is not well predicted. This suggests that another, so far unknown, effect influences the position of some peaks, but not the others.

Version of July 7, 2021– Created July 7, 2021 - 19:45

Chapter 6

CCD images

This section describes measurements of the cavity transmission profiles with a CCD. This camera is capable of measuring the polarization of the modes per pixel. Now it is possible to measure the polarization profiles of different modes. Note that all CCD images are made from the far-field transmission through the 18 micron mirror used before.

6.1 Introduction

The paper by Luk introduced the A and B modes and gave the cavity length where the resonances of these transverse mode are. The prediction was that every ℓ has an A and B mode. The paper by Yu and Luk [12] makes a prediction how these modes look like. Figure 6.1 shows the different polarization profiles predicted by this paper. The theory by Yu and Luk predicts that every ℓ has a unique polarization of every A and B mode. A modes circular like leafs of a clover with the number of leafs equal to $2(\ell - 1)$ for $\ell > 1$. B modes are hyperbolic and have a number of asymptotes equal to $\ell + 1$. This allows us to identify both ℓ and whether a mode is an A or B mode. Since in earlier analysis the different A and B modes are well visible, it is possible to select a single mode and make a CCD picture of this mode. Then from this figure we determine the polarization profile.

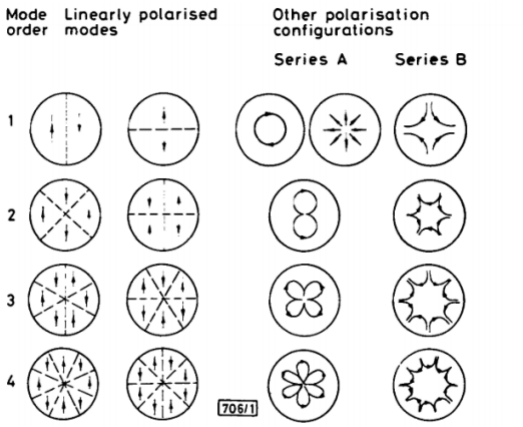

Fig. 1 *Electric field patterns of linearly polarised azimuthal modes and those of other polarisation configurations synthesised from linearly polarised modes of the same order in conventional beam-wave theory*

Figure 6.1: *Figure taken from the paper of Yu and Luk. Here several profiles are visible for p=0. The numbers on the left are the index ℓ.*

6.2 Setup

The top setup in figure 3.1 in chapter 3 shows the setup of the experiment to measure the transmission. The bottom setup in figure 3.1 shows the setup used in this section. This setup is a slightly altered setup compared to the transmission one. The quarter wave plate creates a right handed circular polarized light before it enters the cavity. Output from the cavity is collimated by a 8 mm output lens to 71 cm long a periscope. Then the beam is focused by a 20 cm focal length lens. At the focal length of this lens is a pinhole that filters out unwanted light. The beam is then measured by a CCD camera 7 cm from the pinhole. The CCD camera stores the individual polarizations of one pixel in a 2x2 pixel. Every pixel stores the intensity by a number between 0 and 255. We make a makeshift transmission spectrum by summing over all pixels and then plotting the total intensity against the image number. The result is a plot similar to the PMT transmission plots. However, no advanced corrections are done in this case, because this plot is only used for reference. Using sci-pi find_peaks function, all frames that have a picture of a mode are found. The polarizations are found by calculating the Stokes parameters and plotting the polarization ellipse for several pixels.

The voltage applied on the piezoelectric element is a sawtooth wave with voltage from 6.6 to 9.4 volt. The amplitude is quite high to compensate for the hysteresis of the piezoelectric material. The period of this wave

is 120 seconds. These three numbers allows us to measure at least one full spectral range: 315 nm.

6.3 Results

The transmission spectra and CCD figures are shown in the next few pages. The modes are from N=1 to N=5. The transmission spectrum shown above every set of CCD figures is the total sum over all pixels as a function of the image number. This allows us to correlate the image of the mode and the cavity length. The orange x shows the cavity length where the frames were taken. The transmission spectra and CCD images are from short cavity length to large cavity length.

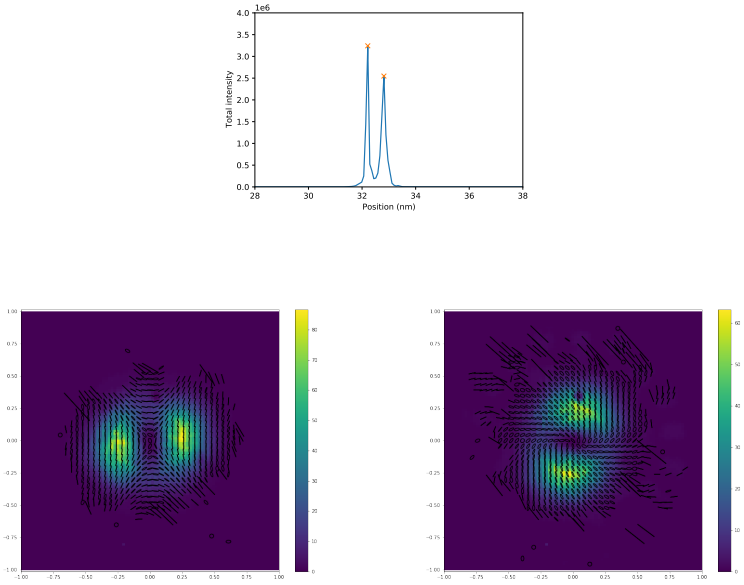

(a) ***(b)***

Figure 6.2: *CCD images of N=1 modes. The black circles show the polarization of the pixels. The polarization profile in figure 6.2a is hyperbolic and is a B1 mode. The polarization profile of figure 6.2b is circular and is an A1 mode.*

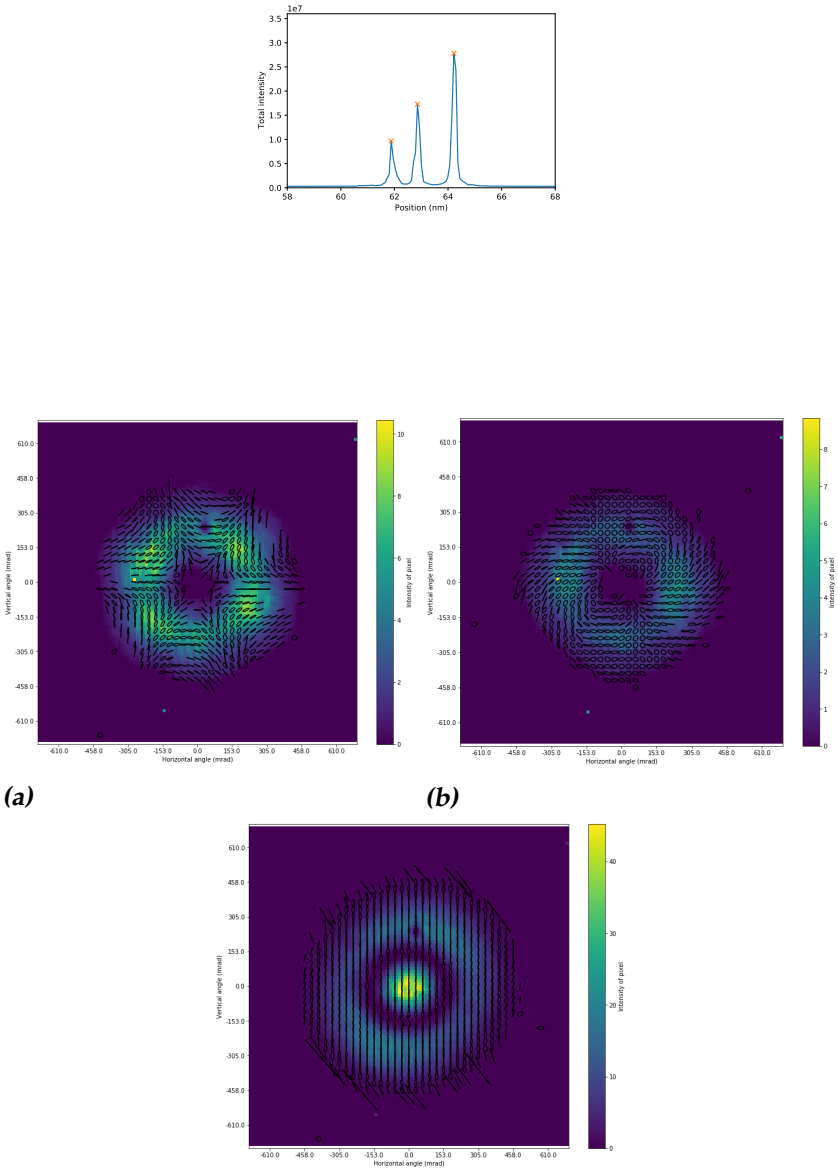

Figure 6.3: *CCD images of N=2 modes. The polarization profile of figure 6.3a is hyperbolic and thus a B2 mode. Figure 6.3b has a lot of circular polarization and is hard to label. It still looks circular, so it might be an A2 mode. Figure 6.3c is an p=1, 0 mode and is fully vertical polarized.*

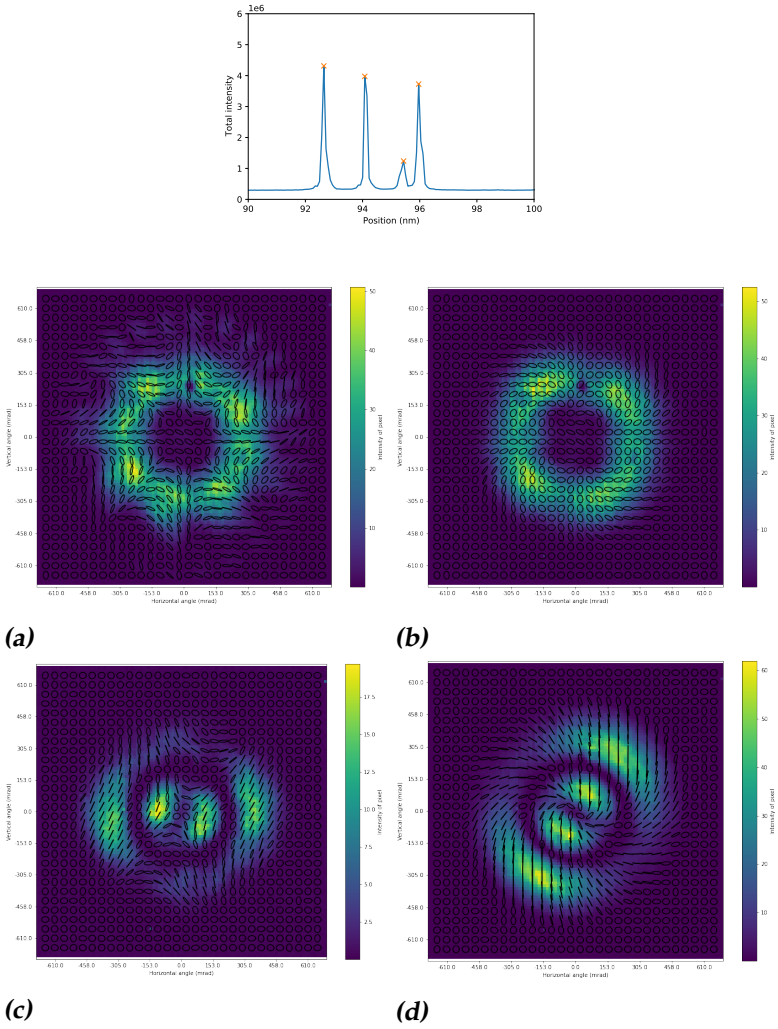

Figure 6.4: *CCD images of N=3 modes. Figure 6.4a is clearly an B3 mode. Figure 6.4b has a lot of circular polarization but resembles mostly an A3 mode. Figure 6.4c is not like any predicted profile, but the hyperbolic nature of the polarization suggests a B mode. Figure 6.4d has the same problem and is likely an A mode.*

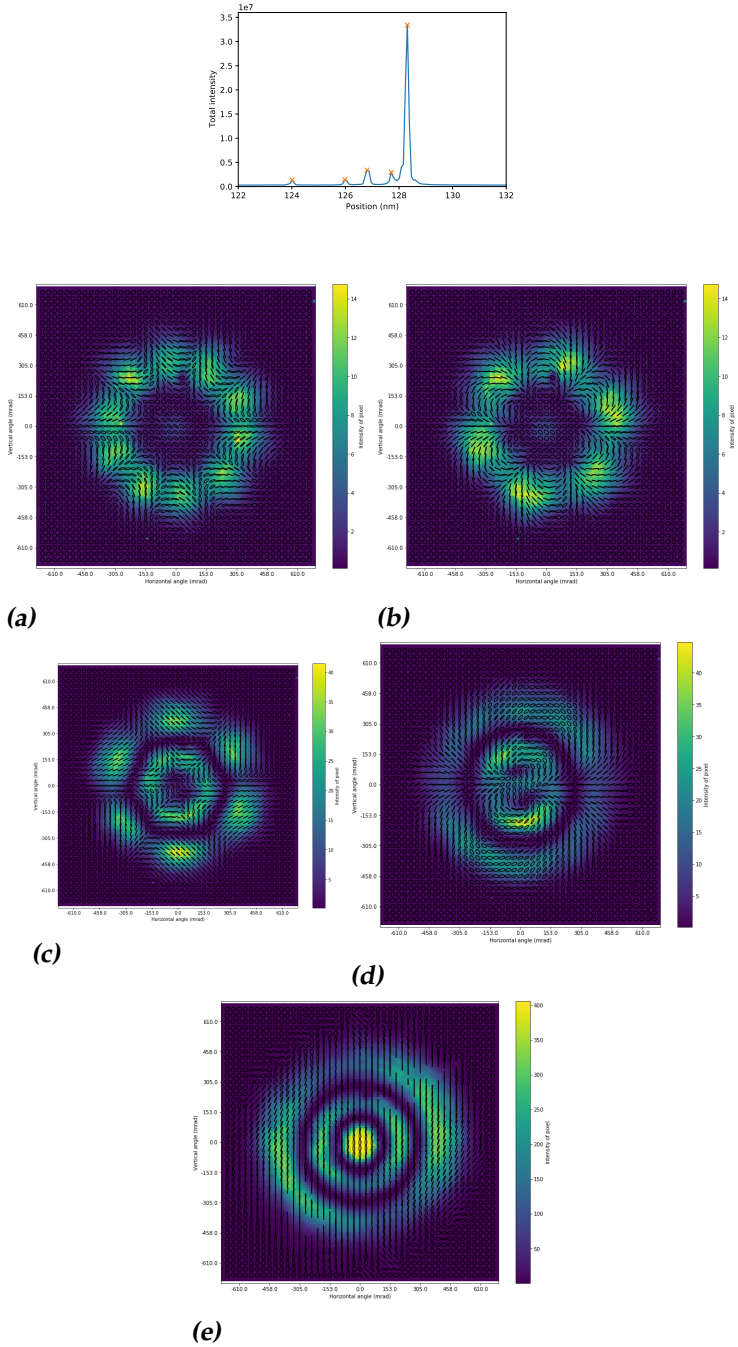

Figure 6.5: *CCD images of N=4 modes. Figure 6.5a and figure 6.5b are respectively a clear B4 and A4 mode. Figure 6.5c and 6.5c are respectively B2 and A2 modes. The final figure 6.5e is an 0 mode and is fully vertically polarized. The circular polarization at the centre is an artifact.*

Version of July 7, 2021– Created July 7, 2021 - 19:45

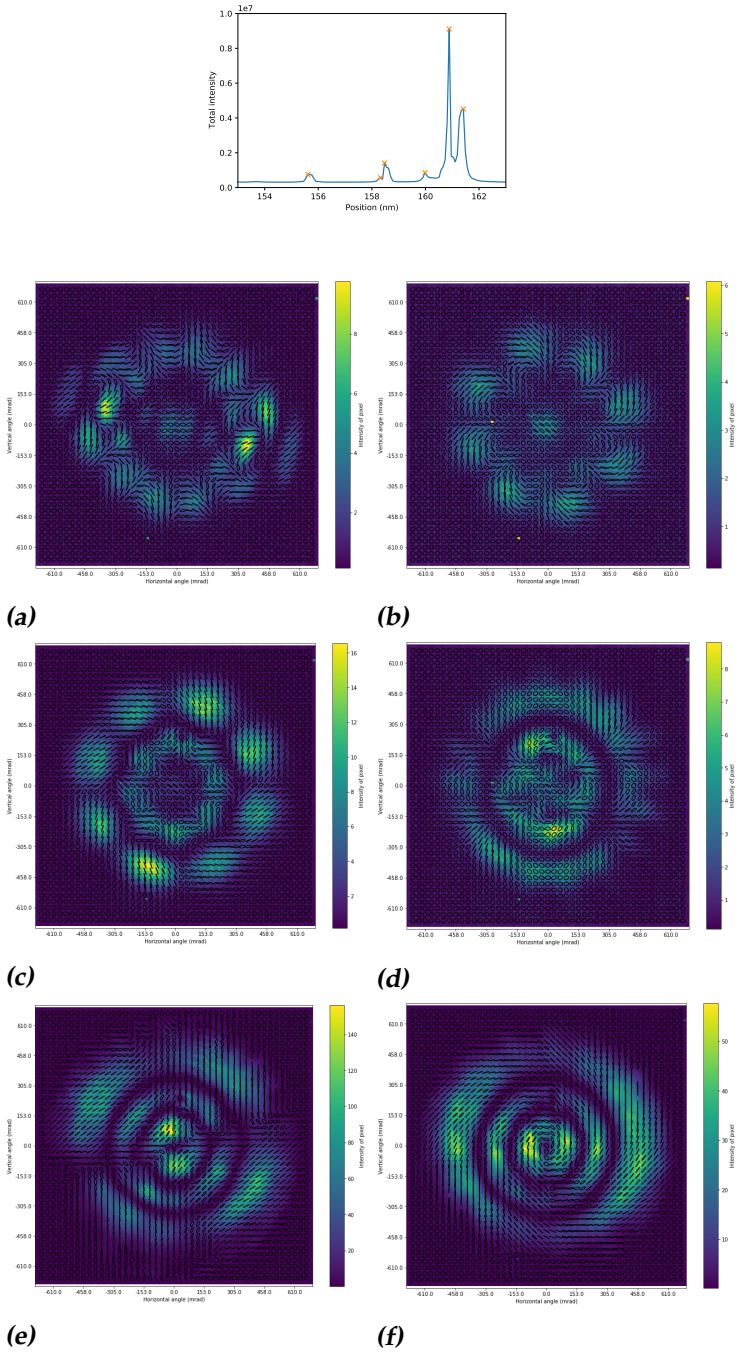

Figure 6.6: *CCD images of N=5 modes. Figure 6.6a and figure 6.6b are B5 and A5 modes. Figure 6.6c is hard to determine, but is certainly a B(3?) mode. Figure 6.6d is an A3 mode. The profile in figure 6.6e is mostly hyperbolic and is an B1 mode. Figure 6.6f is an A1 mode.*

N=4	Theory	B4	B2	A4	0	A2	
	Experiment	B4	A4	B2	A2	0	
N=5	Theory	B5	B3	A5	B1	A3	A1
	Experiment	B5	A5	B3	A3	B1	A1

Table 6.1: *The sequence of A and B modes for N=4 and N=5 that the paper by Yu and Luk predicts and what we measured. The letter shows whether the mode is an A or a B mode, the number shows the index ℓ. The 0 mode is $\ell = 0$, where the A and B resonance have the same cavity length*

6.4 Discussion

The CCD transmission spectra are very similar to the PMT transmission spectra, both in the relative distances between the resonances and the intensity of resonances. The absolute position in cavity length is however not the same. This is because the CCD camera only measured over one free spectral range in contrast to the PMT that scans over 8 free spectral ranges. This means that the CCD transmission spectra have a larger error in the x-axis. This is not a problem, because the transmission spectra meant are to correlate the mode with the position in the transmission spectrum, not for accurate spectral measurements.

The intensity profile of the modes are clearly Laguerre-Gaussian modes. For $\ell \neq 0$, the index p is found by looking at the number of rings and subtract 1. For $\ell = 0$, the index p is equal to the number of rings. The first observation is that the polarization profile in one column look alike. The typical B mode profiles are on the left column and the typical A mode profiles are on the right column. The final $\ell = 0$ mode has an vertical polarization seen in figure 6.3c and 6.5e. Because of symmetry, one would also expect a horizontal polarization for the $\ell = 0$ modes. But these polarizations were not found, suggesting that the setup favours one polarization above the other.

The CCD images supports the theory of Yu and Luk well. Even images with low signal still have very distinct polarization patterns. Especially for N=4 and N=5 the polarization profiles are similar to the predictions in the paper of Yu and Luk. In contrast, some images for N=1 and N=3 are not like the theory. The polarization profiles of N=1 look like somewhat different, whereas the profiles in figure 6.4c and figure 6.4d, N=3, ℓ=1, do look like B and A modes, not exactly like the theory expects.

As seen in the polarization figures, the sequence at which the modes occur, is alternating between B and A modes (ending with a $\ell = 0$ mode if N is even). However, Luk predicts a sequence that starts with two B modes

and ends with two A modes. The table 6.1 compares the order of the N=4 and N=5 modes expected from the theory and the results of the experiment. Note how in the middle every pair of two modes are switched. This reinforces the idea that another effect does move the resonance of some modes, but not for others.

Version of July 7, 2021– Created July 7, 2021 - 19:45

Chapter 7

Atomic Force Microscope

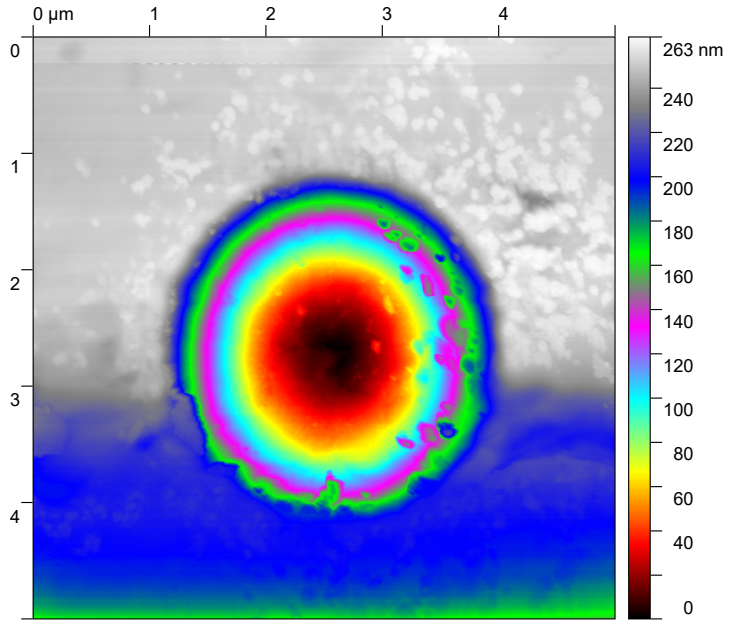

Figure 7.1: *This figure shows the height profile of the 5 µm mirror produced by an AFM. Outside the circle is the planar substrate into which the concave mirror was etched. On the outer side of the mirror are many imperfections, especially on the right hand side. The centre (red/black) is also not fully symmetrical.*

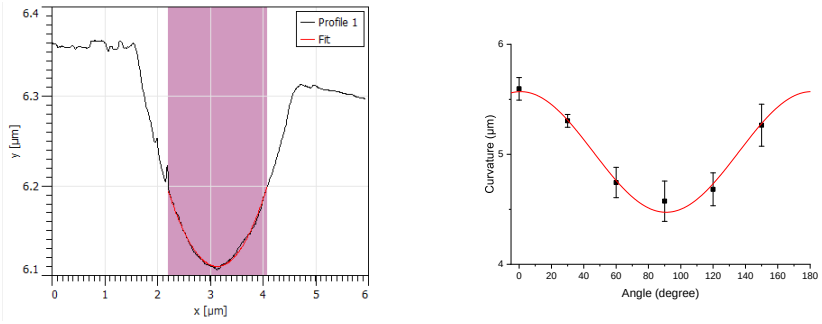

(a) ***(b)***

Figure 7.2: *The left figure shows a cross-section of the mirror shown in figure 7.1. A polynomial of the second order is fitted through the cross-section, inside the purple domain. This returns the radius of curvature the mirror. The right figure shows the radii of curvature for cross section taken under different angles. Figure 7.2b shows that the mirror has a larger radius vertically than horizontally. We then fitted a cosine through the data points.*

7.1 Methods

To find more information about the physical shape of the mirrors, the mirrors were measured with an atomic force microscope. This gives information about the actual radius of curvature and the astigmatism of the mirrors.

Figure 7.1 shows the height profile of the mirrors as measured with an AFM. This height profile is analysed by an AFM analysis program Gwyddion. The first step is to take cross-sections through the height profile. The cross-sections show that the mirrors are approximately parabola that are cut off by a horizontal line. The parabolic part of the cross-sections are fitted with a second-order polynomial. The length is these cross-sections are 2.0 ($\pm$ 0.3) µm. However sometimes a different length is chosen, if there are sudden changes in the height profile. For example in figure 7.2a there is a bump at 2 µm. The selection is then chosen in such a way that this bump is excluded and is still symmetric. We chose to do this because else the fit returned nonphysical radii of curvature and because the centre is the place where the interaction with the beam takes place.

The height z in figure 7.2 is given by equation (7.1).

$$z = \frac{r^2}{2R} \tag{7.1}$$

Where r is the coordinate over the cross section and R is the radius of curvature of the mirror. We measured R for over 6 angles to give a measure

of the astigmatism of the mirror. If the radius of curvature is different for a different angle, then there is astigmatism.

7.2 Results

In figure 7.2b the radii of the mirror is plotted for different angles. A fitted cosine returns the average radius and astigmatism. Astigmatism is here defined as the highest minus the lowest curvature, or in other words, two times the amplitude. The average radius of the 5 micron mirror, is $R_{av} = 5.06\ (\pm 0.04)$ µm. The maximum radius is $R_1 = 5.4\ (\pm 0.1)$ µm and the minimum radius is $R_2 = 4.7\ (\pm 0.1)$ µm. $\Delta R = R_1 + R_2 = 0.70\ (\pm 0.14)$ µm.

7.3 Discussion

Now with the optical analysis and the AFM measurements, it is possible to compare both. The AFM measures $R_{av} = 5.06$ µm and $\Delta R = 0.70$ µm. Then $\eta = \frac{0.70}{2*5.06} = 0.07$. Equation (7.2) shows again the equation given by the paper by Uphoff.

$$\Delta L = \frac{\lambda}{2\pi k R_{av}} \eta \tag{7.2}$$

Substituting R_{av} and η, returns that the predicted splitting is $\Delta L = 0.14$ nm. The optical data showed that $\Delta L = 0.085$ nm. The measured average radius of curvature is close to what the arcsin fit predicts. The splitting of the fundamental modes is also close to what Uphoff predicts. However, the distance is still off by about 60%. The likely cause of this is the large errors in the fundamental mode distances and the error in the AFM measurement.

There was unfortunately not enough time to do an in-depth analysis of the 18 micron mirror, but a quick look at the mirror found a very low astigmatism in the order of $\eta = 0.03$. That explains why we only found non-paraxial splitting and no splitting due to astigmatism.

Version of July 7, 2021– Created July 7, 2021 - 19:45

Chapter 8

Concluding Discussion

In this thesis we conclude that the fine structure is clearly visible for both the 5 micron and the 18 micron cavities. We also can identify the polarization profiles of the higher-order modes. Combining both results, we correlate the resonant cavity lengths with labeled modes (q, N, $\pm\ell$). In addition, we find the fundamental mode splitting of a 5 micron mirror and have the AFM measurements of this mirror. We compare the findings with three theoretical predictions: (i) a prediction of the spectral fine structure by Luk [8], (ii) a prediction of the polarization profiles of the modes by Yu and Luk [12], and (iii) a prediction of the frequency splitting between the two polarized fundamental modes.

The examination of spectral fine structure shows that the number of resonances that we measure for each (q, N) group is equal to N+1 for most measurements. However, the distance between transverse modes is not always what the paper by Luk [8] predicts. For some modes the distance is very close to the predicted distance, but for other modes it is off by an order of magnitude.

The paper by Yu and Luk [12] also predicts polarization profiles for the transverse modes. For most modes the measured polarization profile is the same as the predicted polarization profile. This allows us to identify modes and look in what order modes occur for a (q, N) group. The order of modes is not the same order Luk [8] predicts (table 6.1). All pairs of two modes (with the exception of the first B mode) are switched around. This is likely the reason why the measured distances between modes do not always match what is predicted.

The incorrect spacing between, and the order of the modes suggests that the non-paraxial models are correct, but insufficient do fully describe the fine structure of a Fabry–Perot interferometer. There might be an addi-

tional effect that moves the resonant cavity length of some modes but not others.

The predicted frequency splitting of the fundamental modes could be clearly observed only in measurement series 5g. AFM measurements of the mirror shape confirms the origin of the observed splitting of fundamental modes. Although the margin of error is high, the AFM measurement shows that Uphoff [3] predicts the splitting caused by astigmatism correctly.

Bibliography

[1] Greuter et al. A small mode volume tunable microcavity: Development and characterization. *Applied Physics Letters*, 12(105), 2014.

[2] Julia Benedikter et al. Transverse-mode coupling effects in scanning cavity microscopy. *New Journal of Physics*, 21:103029, 2019.

[3] Manuel Uphoff et al. Frequency splitting of polarization eigenmodes in microscopic fabry –perot cavities. *New Journal of Physics*, 17, 2015.

[4] David H. Foster, Andrew K. Cook, and Jens U. Nöckel. Degenerate perturbation theory describing the mixing of orbital angular momentum modes in fabry-perot cavity resonators. *Phys. Rev. A*, 79:011803, Jan 2009.

[5] John L. Hall, Jun Ye, and Long-Sheng Ma. Measurement of mirror birefringence at the sub-ppm level: Proposed application to a test of qed. *Phys. Rev. A*, 62:013815, Jun 2000.

[6] Dustin Kleckner, William T. M. Irvine, Sumant S. R. Oemrawsingh, and Dirk Bouwmeester. Diffraction-limited high-finesse optical cavities. *Phys. Rev. A*, 81:043814, Apr 2010.

[7] C. Koks and M. P. van Exter. Microcavity resonance condition, quality factor, and mode volume are determined by different penetration depths. *Optics Express*, 29(5):6879, Feb 2021.

[8] Kwai-Man Luk. Improvement in the resonant formula of a spherical fabry–perot resonator with unequal mirrors. *J. Opt. Soc. Am. A*, 3(1):3–6, Jan 1986.

[9] Siegman. *Lasers*. 1986.

[10] Svelto. *Principles of lasers*. Springer, 2010.

[11] Kerry J Vahala. Optical microcavities. *Nature*, 424(6950):839–846, August 2003.

[12] P.K. Yu and K.M. Luk. High-order azimuthal modes in the open resonator. *Electronics Letters*, 14(16):539–541, 1983.